ELSEVIER

Biophysical Chemistry 110 (2004) 179–190

Biophysical Chemistry

www.elsevier.com/locate/bpc

Effects of inositol 1,4,5-trisphosphate receptor-mediated intracellular stochastic calcium oscillations on activation of glycogen phosphorylase

Dan Wu[a,*], Ya Jia[a], Anvar Rozi[a,b]

[a] *Department of Physics, Central China Normal University, Wuhan 430079, Hubei, PR China*
[b] *Department of Physics, Kashgar Teachers College, Kashgar 840007, Xinjiang, PR China*

Received 29 November 2003; received in revised form 11 February 2004; accepted 12 February 2004
Available online 27 April 2004

Abstract

In various cell types cytosolic calcium (Ca^{2+}) is an important regulator. The possible role of Ca^{2+} release from the inositol 1,4,5-trisphosphate (IP_3) receptor channel in the regulation of the phosphorylation–dephosphorylation cycle process involved in glycogen degradation by glycogen phosphorylase have theoretically investigated by using the Li–Rinzel model for cytosolic Ca^{2+} oscillations. For the case of deterministic cytosolic Ca^{2+} oscillations, there exists an optimal frequency of cytosolic Ca^{2+} oscillations at which the average fraction of active glycogen phosphorylase reaches a maximum value, and a mutation for the average fraction of active glycogen phosphorylase occurs at the higher bifurcation point of Ca^{2+} oscillations. For the case of stochastic cytosolic Ca^{2+} oscillations, the fraction of active phosphorylase is strongly affected by the number of IP_3 receptor channels and the level of IP_3 concentration. Small number of IP_3 receptor channels can potentiate the sensitivity of the activity of glycogen phosphorylase. The average frequency and amplitude of active phosphorylase stochastic oscillations are increased with the level of increasing IP_3 stimuli. The various distributions for the amplitude of active glycogen phosphorylase oscillations in parameters plane are discussed.
© 2004 Elsevier B.V. All rights reserved.

Keywords: IP_3 receptor; Calcium oscillations; Fraction of active glycogen phosphorylase

1. Introduction

Intracellular Ca^{2+} is a primary regulator with variety of cell functions, for example, early response to injury of brain tissue [1], neurotransmitter release [2], synaptic plasticity [3], gene expression [4], and cell death [5], etc. Phosphorylation–dephosphorylation cascades represent one of the most exquisite modes of cellular regulation. A prototypic example of phosphorylation–dephosphorylation cascade involved in metabolic regulation is the one controlling the balance between glycogen synthesis and degradation. The coordinated changes in the phosphorylation status of glycogen synthase and glycogen phosphorylase are under hormonal control through the activation of protein kinases by cyclic AMP (cAMP) and cytosolic Ca^{2+}. The control of glycogen phosphorylase by cytosolic Ca^{2+}

* Corresponding author. Tel.: +86-027-62714728; fax: +86-027-67866070
E-mail addresses: wud@phy.ccnu.edu.cn (D. Wu), jiay@phy.ccnu.edu.cn (Y. Jia).

0301-4622/$ - see front matter © 2004 Elsevier B.V. All rights reserved.
doi:10.1016/j.bpc.2004.02.002

provides a prototypic example to study the impact of Ca^{2+} oscillations on cellular regulation.

Recently, Gall et al. [6] have studied theoretically the effects of simple cytosolic Ca^{2+} oscillations on the activation of glycogen phosphorylase controlled by the phosphorylation–dephosphorylation cycle based on bicyclic cascade model proposed by Cárdenas and Goldbeter [7] in hepatocytes. It is found that cytosolic Ca^{2+} oscillations reduce the threshold for the activation of the enzyme, that the cytosolic Ca^{2+} oscillations can potentiate the response to a hormonal stimulation, and that cytosolic Ca^{2+} oscillations in hepatocytes can contribute to increase the efficiency and specificity of cellular signaling as shown experimentally for gene expression in lymphocytes [4]. Rozi and Jia [8] have investigated the effects of complex cytosolic Ca^{2+} oscillations on the regulation of the activation of glycogen phosphorylase. It is predicted that an average level of the fraction of active phosphorylase is nearly independent of the level of external stimulation increasing during the cytosolic Ca^{2+} bursting oscillations.

Cytosolic Ca^{2+} shows complex spatio-temporal oscillatory profiles in a large number of cell types. A number of mathematical models have been proposed. Some assume that IP_3 is necessarily oscillatory, or assume the existence of two pools for Ca^{2+} and emphasize the effect of Ca^{2+}-induced Ca^{2+}-release. Some assume that inhibition of Ca^{2+}-release by endoplasmic reticulum (ER) luminal calcium or by cytosolic calcium is crucial, and some even assume the involvement of ER membrane potential. These models that give qualitative description of how oscillations might occur were developed before important features of IP_3- and Ca^{2+}-gated channel opening were characterized. It has been found that the release of Ca^{2+} from intracellular pools can be mediated by two types of receptor channel proteins, the IP_3 receptor (IP_3R) [9,10] and the ryanodine receptor (RyR) [11–13], which have quite different gating properties and single channel conductances. The generation of cytosolic Ca^{2+} oscillations does not require the presence of both types of Ca^{2+}-release channel. In addition, it has been observed that the Ca^{2+}-release channels are spatially organized in clusters. The collective opening and closing of several calcium release channels in a cluster causes Ca^{2+} puffs or sparks observed in experiments [14–18].

The first theoretical model for agonist-induced cytosolic Ca^{2+} oscillations based on microscopic kinetics of IP_3 and cytosolic Ca^{2+} gating of the IP_3R was proposed by De Young and Keizer [19], which provides good agreement with experimental recordings of channel opening. This model requires nine variables for IP_3 receptor. Since the full De Young–Keizer model is symmetric in some of the three binding processes (i.e. IP_3 binding, Ca^{2+} binding to activation site, and Ca^{2+} binding to inactivation site) and the IP_3 binding is at least 200 times faster than other binding processes, a much simpler two variables model based on the De Young–Keizer model was proposed by Li and Rinzel [20]. The Li–Rinzel model is analogous in form to the Hodgkin–Huxley formalism for electrical excitability of neuronal plasma membrane [21]. Recently, a stochastic version of Li–Rinzel model is proposed by Shuai and Jung [22].

In this article, we employ Li–Rinzel model for cytosolic Ca^{2+} oscillations (including deterministic and stochastic version) to simulate the possible role of calcium release from the IP_3R in the regulation of the phosphorylation–dephosphorylation cycle process involved in glycogen degradation by glycogen phosphorylase, since this process plays a vital role in the regulation of glycaemia, and in providing glucose for the organism between feeding in hepatocytes (for review see Ref. [23]). In particular, we indeed explore theoretically the effects of different numbers of IP_3Rs and different levels of IP_3 stimuli on the activation of glycogen phosphorylase by stochastic cytosolic Ca^{2+} oscillations. It should be pointed out that the random Ca^{2+} signals discussed are localized signals since the stochastic Li–Rinzel model is applied for the localized calcium signals released from the clustered IP_3Rs channels. Moreover, the channels of Ca^{2+} are assumed [22] to be close enough so that cytosolic Ca^{2+} concentration can be considered homogeneous throughout the cluster, and the diffusion between cluster and environment is neglected without accounting for spatial aspects of the formation and collapse of localized Ca^{2+} elevations.

2. Model

The function of glycogen phosphorylase is to govern glycogen degradation. The enzyme acts as a

sensor of blood glucose level, liberating glucose from stored glycogen as needed. The dynamics of the Ca^{2+}-associated phosphorylation cycle involves glycogen phosphorylase: glycogen phosphorylase is converted from the inactive *b*-form into the active *a*-form by phosphorylase kinase, and is inactivated by a phosphatase. Phosphorylase kinase is a hexadecamer composed of four different subunits ($\alpha_4\beta_4\gamma_4\delta_4$). The δ subunit is identical to calmodulin and mediates the Ca^{2+}-sensitivity of phosphorylase kinase [24]. The minimal model based on the bicyclic cascade model proposed by Cárdenas and Golbeter [7] for the activation of glycogen phosphorylase taking into account the regulation by cytosolic Ca^{2+} has been proposed by Gall et al. [6]. The balance equation governing the time evolution of the fraction of active glycogen phosphorylase (X) is given by:

$$\frac{dX}{dt} = V_1(Z)\frac{1-X}{K_1(Z)+1-X} - \frac{V_{M2}(1+\alpha G/(K_{a1}+G))X}{K_2/(1+G/K_{a2})+X}, \quad (1)$$

with

$$V_1(Z) = V_{M1}\left(1+\gamma\frac{Z^4}{K_{a5}^4+Z^4}\right),$$

$$K_1(Z) = \frac{K_1^1}{1+Z^4/K_{a6}^4}, \quad (2)$$

where Z and G represent the intracellular concentration of Ca^{2+} and glucose, respectively. In this model, it has been assumed that glucose activates phosphorylase phosphatase (of maximum rate V_{M2} and normalized Michaelis constant K_2) by decreasing the K_m of enzyme, with an activation constant K_{a2}, and that glucose further activates the enzyme by enhancing its maximum rate by a multiplicative factor α, with an activation constant K_{a1}. Moreover, it is also assumed that Ca^{2+} activates the phosphorylase kinase (of maximum rate V_{M1} and normalized Michaelis constant K_1) by decreasing the K_m of the enzyme, with an activation constant K_{a6}, and that Ca^{2+} further activates the enzyme by enhancing its maximum rate by a multiplicative factor γ, with an activation constant K_{a5}. In order to study the regulation by cytosolic Ca^{2+} of the glycogen phosphorylase, a constant cAMP level has been assumed, and the rates of phosphorylation of glycogen phosphorylase kinase by the cAMP-dependent kinases are taken as constant parameters. The values of these parameters [6,8] are G=10.0 mM, $K_1^1 = 0.1$, K_2=0.2, K_{a1}=K_{a2}=10.0 mM, K_{a5}=K_{a6}=0.5 μM, α=γ=9.0, V_{M1}=1.5 min^{-1}, V_{M2}=0.6 min^{-1}.

2.1. Deterministic Li–Rinzel model

The De Young–Keizer model is the first theoretical model for agonist-induced cytosolic Ca^{2+} oscillations based on microscopic kinetics of IP_3 and Ca^{2+} gating of the IP_3R [19]. This model assumes that three equivalent and independent subunits are involved in conduction in an IP_3R. Each subunit has one IP_3 binding site (*m* gate), and two Ca^{2+} binding sites (one for activation (*n* gate), the other for inhibition (*h* gate)). Thus, each subunit may exist in eight states with transitions governed by second-order and first-order rate constants. Only the state with one IP_3 and one activating Ca^{2+} bound contributes to the subunit's open probability. All three subunits must be in this state for the channel to be open. Although the model is unique in giving in detail gating kinetics, the number of variables is relatively high. This model involves eight variables plus the concentration of IP_3 as a control parameter. Li and Rinzel [20] showed that the full De Young–Keizer model is symmetric in some of the binding processes and that the IP_3 binding is at lease 200 times faster than the Ca^{2+} activation binding, while the Ca^{2+} activation binding is at least 10 times faster than the Ca^{2+} inactivation binding and the change rate of $[Ca^{2+}]$ during oscillations. Therefore, the nine-variables De Young–Keizer model can be reduced to two-variables model:

$$\frac{dZ}{dt} = J_{rel} - J_{pump}, \quad (3)$$

$$\frac{dh}{dt} = \alpha_h(1-h) - \beta_h h, \quad (4)$$

where J_{rel} is calcium release flux from ER to the intracellular space, and J_{pump} is calcium flux pumped

from the intracellular space into the ER. The expressions for these fluxes are:

$$J_{\text{rel}} = c_1\left(v_1 m_\infty^3 n_\infty^3 h^3 + v_2\right)(Z_{ER} - Z), \tag{5}$$

$$J_{\text{pump}} = v_3 \frac{Z^2}{k_3^2 + Z^2}, \tag{6}$$

with

$$m_\infty = \frac{P}{P + d_1},$$

$$n_\infty = \frac{Z}{Z + d_5},$$

$$\alpha_h = a_2 d_2 \frac{P + d_1}{P + d_3},$$

$$\beta_h = a_2 Z,$$

P denotes the intracellular concentration of IP_3, and v_1 and v_2 are the rate constants of maximal IP_3R-mediated release flux and of a small leak flux, respectively. α_h and β_h are the opening rate and closing rate for h gates, respectively. In above model, the fast variables m, n have been replaced by their quasi-equilibrium values m_∞ and n_∞, and a conservation of the total cellular Ca^{2+} implies the constraint: $c_0 = Z + c_1 Z_{ER}$. The values of these parameters [20,22] are: c_0=2.0 μM, c_1=0.185, v_1=360.0 min^{-1}, v_2=6.6 min^{-1}, v_3=54.0 μM min^{-1}, k_3=0.1 μM, d_1=0.13 μM, d_2=1.049 μM, d_3=0.9434 μM, d_5=0.08234 μM, a_2=12.0 μM^{-1} min^{-1}. Parameter P is considered as a control parameter.

2.2. Stochastic Li–Rinzel model

Eqs. (3) and (4) describe the deterministic behavior of cytosolic Ca^{2+} averaged for a large number of channels. The small number of IP_3R channels in a single cluster suggests that a stochastic formulation of these equations is necessary if calcium release from a single cluster is considered. Thus, there is an increasing interest for the theoretical discussion on the stochastic dynamics of local Ca^{2+} release [25–30]. The deterministic Li–Rinzel model (Eqs. (3) and (4)) is a structure analogous to the famous Hodgkin–Huxley formalism for electrical excitability of neuronal plasma membrane [21]. In particular, fast activation and slow inactivation by Ca^{2+} of the IP_3R channel become analogous to gating by membrane potential of the plasma membrane Na^+ channel [20]. Following the deterministic Li–Rinzel model, we only consider the stochastic opening and closing process for gate h here. There are several ways to simulate this stochastic scheme (for detail see Ref. [22]). A widely applied approach is to account for the number of ionic channels in each state of the kinetic model [31–33]. The IP_3R channel can exist in four different states, and the kinetic scheme describing the behavior of this channel is given by:

$$[n_0] \underset{\beta_h}{\overset{3\alpha_h}{\rightleftharpoons}} [n_1] \underset{2\beta_h}{\overset{2\alpha_h}{\rightleftharpoons}} [n_2] \underset{3\beta_h}{\overset{\alpha_h}{\rightleftharpoons}} [n_3] \tag{7}$$

where $[n_i]$ is the number of the channel with i open gates, and hence $[n_3]$ labels the open state of the IP_3R channel. The total population of channels in each of their possible states will be tracked with time. The expression for the calcium release flux replacing Eq. (5) is given by [22]:

$$J_{\text{rel}} = c_1\left(v_1 m_\infty^3 n_\infty^3 \frac{N_{h-\text{open}}}{N} + v_2\right)(Z_{ER} - Z), \tag{8}$$

where N and $N_{h\text{-open}}$ indicate the total number of IP_3R channels and the number of h-open channels, respectively. $N_{h\text{-open}}/N$ is the h-open fraction, replacing h^3 in Eq. (5) of the deterministic model. A change in parameter N is implicitly associated with a change in the Ca^{2+} flux through channels.

To simulate the effects of different numbers of IP_3R channel and different levels of IP_3 stimuli on the activation of glycogen phosphorylase by stochastic cytosolic Ca^{2+} oscillations, Eqs. (1), (3) and (4) were integrated by the forward Eular algorithm with a time step of 0.001 min. In each calculation, the time evolution of the system lasted 1000 min after transient behavior was discarded.

3. Effects of IP_3 receptor-mediated cytosolic Ca^{2+} oscillations on activation of glycogen phosphorylase

In the deterministic Li–Rinzel model (i.e. J_{rel} is given by Eq. (5)), the variation of concentration of IP_3

gives rise to intracellular Ca^{2+} oscillations, and the frequency of cytosolic Ca^{2+} oscillations and the average cytosolic Ca^{2+} concentration ($\langle Z\rangle$) are increased with the IP_3 stimulation level increasing [20]. The bifurcation diagram for the intracellular Ca^{2+} concentration (Z) is plotted in Fig. 1a (the dashed line).

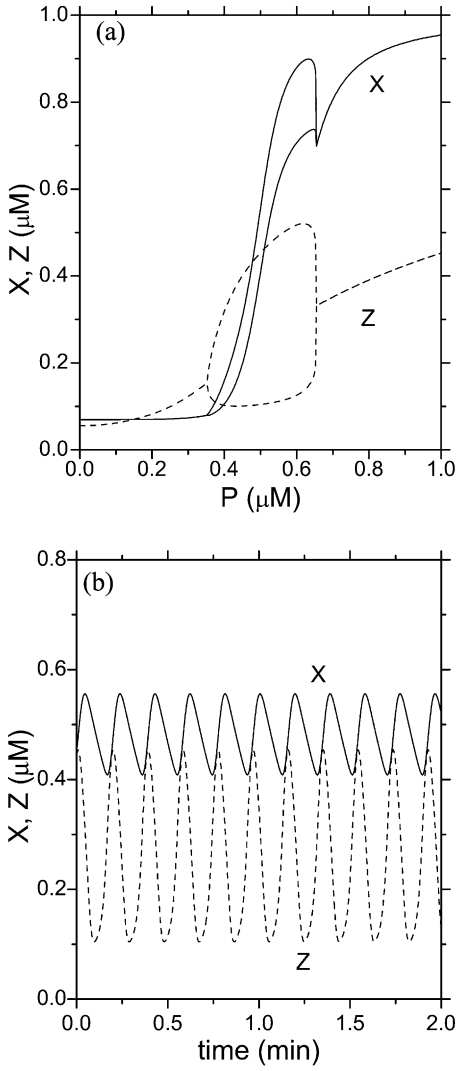

Fig. 1. (a) The bifurcation diagrams of X (solid line) and Z (dashed line) are plotted against the stimulus parameter, P. Within the range of P values giving rise to oscillations, both the maximum and the minimum of X and Z in the course of oscillations are drawn. (b) Time courses of X (solid line) and Z (dashed line) at a given level of P=0.5 μM.

Under the regulation of cytosolic Ca^{2+} oscillations, the fraction of active glycogen phosphorylase (X) can also oscillate in the range of cytosolic Ca^{2+} oscillations (see the bifurcation diagram for X in Fig. 1a, the solid line). In other words, the cytosolic Ca^{2+} oscillations induce the activation of glycogen phosphorylase oscillating. The time courses of Z and X are shown in Fig. 1b when P=0.5 μM at which cytosolic calcium oscillates. As can be expected from the regulations considered, the peaks in cytosolic Ca^{2+} precede the peaks in fraction of active phosphorylase [6,8].

To explore the effects of different IP_3 stimuli on the activation of glycogen phosphorylase, the average level of fraction of active phosphorylase ($\langle X\rangle$) as a function of IP_3 concentration (P) is plotted in Fig. 2a. It can be found that, in the domain of cytosolic Ca^{2+} oscillations, $\langle X\rangle$ is increased with P increasing firstly, and then has a little decrease. There exists an optimal frequency of cytosolic Ca^{2+} oscillations (or an optimal IP_3 stimuli, P=0.635 μM) at which the average fraction of active glycogen phosphorylase reaches a maximum value (see point A in Fig. 2a). It is interesting to notice that the average fraction of active phosphorylase drops suddenly from high level to low value when the cytosolic Ca^{2+} oscillation is over (see point B at which P=0.655 μM in Fig. 2a). It means that the average fraction of active glycogen phosphorylase is very sensitive to the cytosolic calcium oscillations at the higher bifurcation point of Ca^{2+} oscillations. In Fig. 2b, the relationship between $\langle X\rangle$ and $\langle Z\rangle$ with variable P (P varies from 0 to 1 μM) shows a steep sigmoidal nature [6]. This result is a direct consequence of the saturation of the converter enzymes by their substrates, leading to a phenomenon known as 'zero-order ultrasensitivity' [34], and of the cooperativity in the kinase activation by Ca^{2+} [35]. We compare $\langle X\rangle$ activated by Ca^{2+} oscillations (solid star) with $\langle X\rangle$ activated by a sustained Ca^{2+} level in Fig. 2b, in which the solid line (i.e. the stable steady-state value) is obtained by setting dX/dt=0 in Eq. (1). It shows that cytosolic Ca^{2+} oscillations reduce the threshold for the activation of the enzyme, or potentiate the cell response.

In the stochastic cytosolic Ca^{2+} model (i.e. J_{rel} is given by Eq. (8)), it has been shown [22] that, even

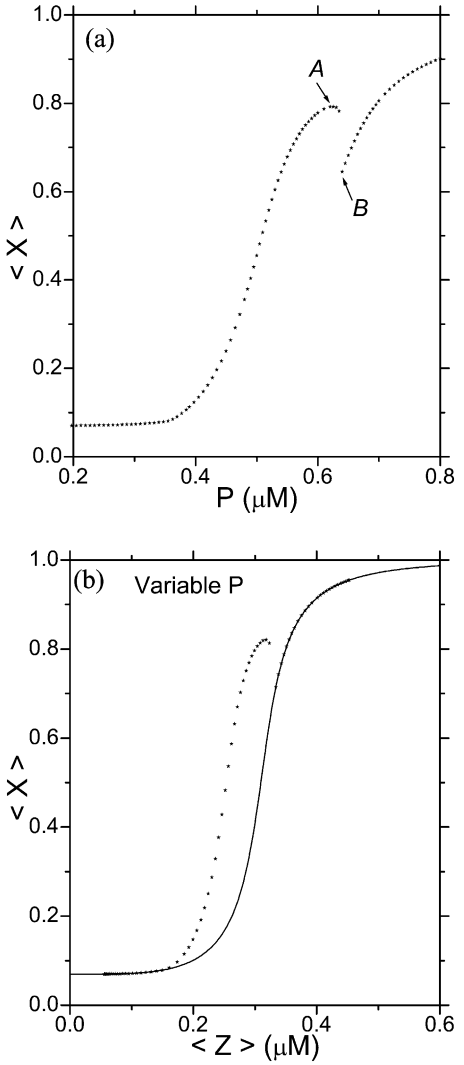

Fig. 2. (a) The average value of X ($\langle X\rangle$) are plotted against P. Point A corresponds to the maximum value of $\langle X\rangle$. Point B corresponds to P=0.655 μM, which is the higher bifurcation point for Z in the deterministic case (see Fig. 1a). (b) $\langle X\rangle$ vs. $\langle Z\rangle$ (solid star) with variable P (P varies from 0 to 1 μM). The line is the response of X to a stimulation by a sustained Ca^{2+} level (which is obtained by setting $\dot{X} = 0$ in Eq. (1)).

not in the range of cytosolic Ca^{2+} oscillations as shown in Fig. 1a, intracellular concentration of calcium can oscillate stochastically due to the random opening and closing of IP_3- and Ca^{2+}-gated channels. Fig. 3 gives the bifurcation diagrams for the stochastic case, which plots both the maximum and minimum of X and Z in the process of their stochastic oscillations. We can see that, although the features of the deterministic bifurcation diagrams are well reproduced when the total number of channels is large (e.g. N=100 000), the oscillation range in the stochastic case is larger than that one in the deterministic case. Now a question to be raised is how the stochastic cytosolic Ca^{2+} oscillations affect the activation of glycogen phosphorylase, or what are the effects of different numbers of IP_3Rs and different IP_3 stimuli on the activation of glycogen phosphorylase by cytosolic Ca^{2+} stochastic oscillations?

When the intracellular concentration of IP_3 is fixed at P=0.3 μM at which cytosolic Ca^{2+} oscillations do not occur for the deterministic case, we show the temporal evolutions of X and Z for different total numbers of IP_3R channel (N) in Fig. 4. Fig. 4a demonstrates that the fraction of active phosphorylase oscillates stochastically with large amplitude by the regulation of cytosolic Ca^{2+} stochastic oscillations for the small total number of IP_3R channels. With the increasing of the total number of IP_3R channels, the oscillation amplitude of the fraction of active phosphorylase becomes smaller. The oscillations in the fraction of active phosphorylase vanish when N is very large (e.g. N=1000 in Fig. 4d). However, when

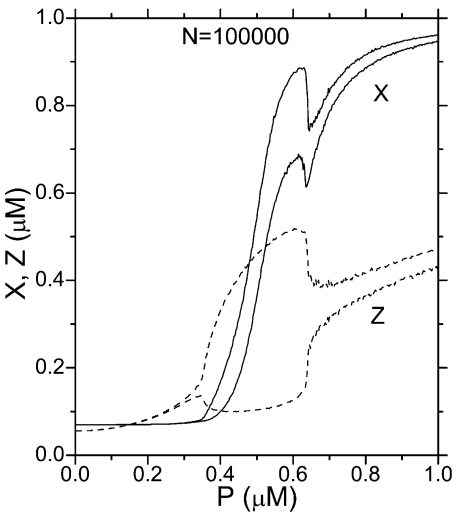

Fig. 3. The bifurcation diagram of X (solid line) and Z (dashed line) as a function of P for the stochastic case (N=100 000).

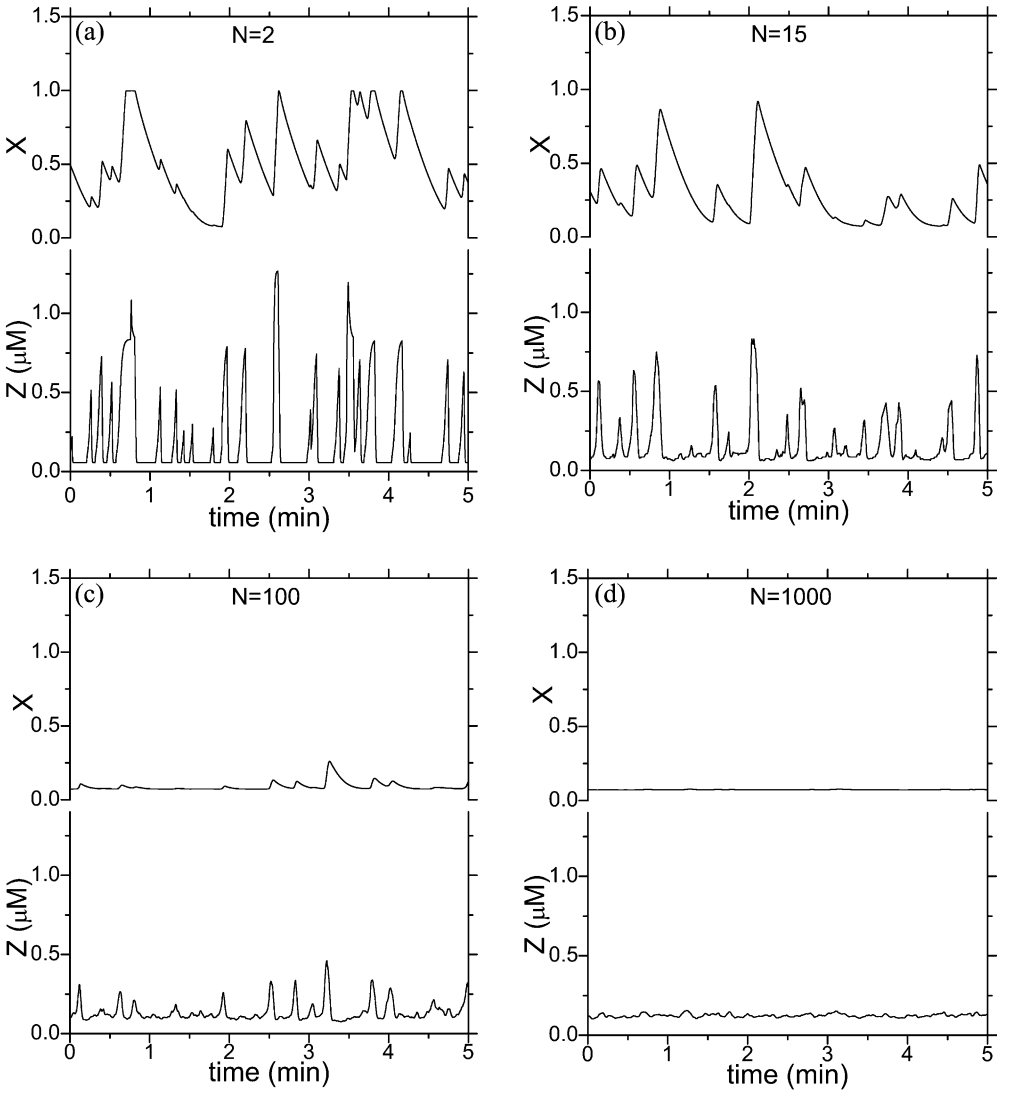

Fig. 4. Time course of X is compared with the associated time courses of Z at P=0.3 μM level for different total channel number: (a) N=2, (b) N=15, (c) N=100, and (d) N=1000.

the total number of IP_3R channels is fixed, for example, N=20, the temporal evolutions of X and Z for different intracellular concentration of IP_3 are shown in Fig. 5. It is found that there is no variation (or oscillations) in the fraction of active phosphorylase at the low level of IP_3 stimuli (e.g. P=0.2 μM in Fig. 5a). However, under the regulation of cytosolic Ca^{2+} random oscillations, the average frequency and amplitude in the stochastic oscillations of the fraction of active phosphorylase are increased with the increasing of the IP_3 level (see Fig. 5b–d).

Figs. 4 and 5 also show that the oscillating amplitude and frequency of the fraction of active phosphorylase are determined by the concentration of cytosolic Ca^{2+} and its oscillating frequency. The time scale of cytosolic Ca^{2+} stochastic oscillation process is faster than that of active phos-

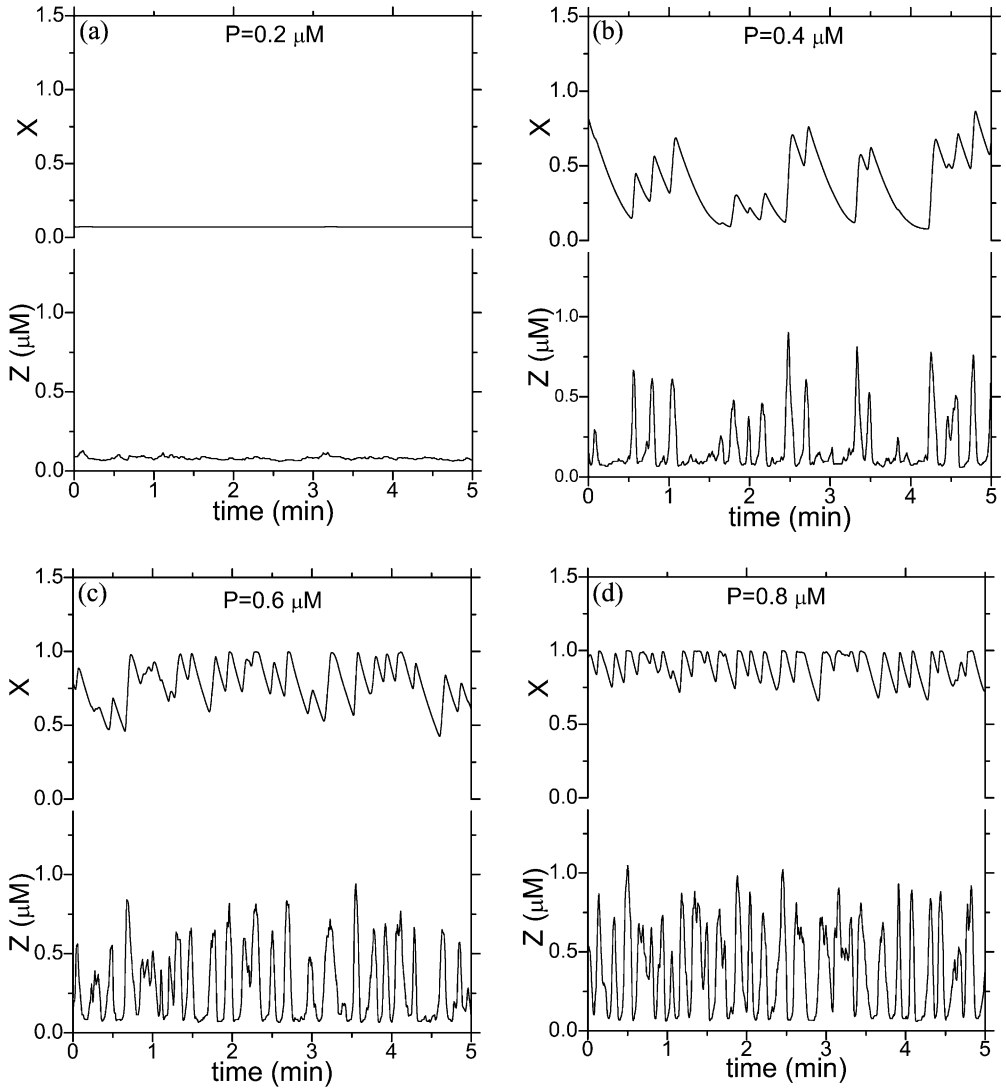

Fig. 5. Time courses of X and Z at a given channel number N=20 for P=0.2 μM (a), P=0.4 μM (b), P=0.6 μM (c), and P=0.8 μM (d).

phorylase. Therefore, significant dephosphorylation of glycogen phosphorylase is only possible when the time interval between two successive Ca^{2+} spikes is large enough. At higher frequency of Ca^{2+} oscillation, dephosphorylation between successive Ca^{2+} spikes is not complete and higher $\langle X\rangle$ levels can be maintained. The phenomenon that $\langle X\rangle$ levels depend on the frequency of cytosolic Ca^{2+} oscillations is called as frequency encoding [6].

The steep sigmoidal nature is also obtained in the stochastic version (see Fig. 6a). It shows that the threshold of $\langle Z\rangle$ for activation of phosphorylase depends on the total number of IP_3R channel. The smaller the total number of IP_3R channel is, the lower the threshold of $\langle Z\rangle$ for activation of phosphorylase is. Because the small IP_3Rs channels cluster can induce large fluctuations in cytosolic Ca^{2+} concentration, the level of Ca^{2+} sometimes goes above the level required for activation of the

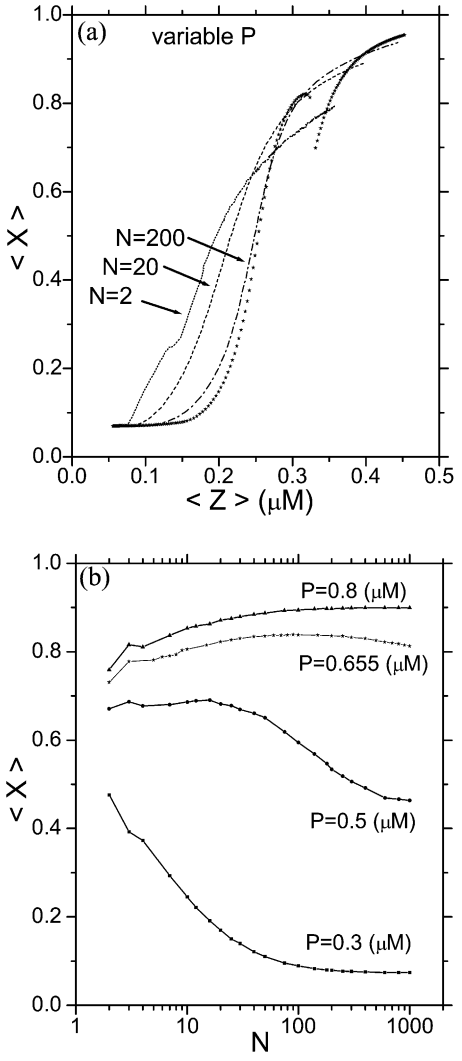

Fig. 6. (a) $\langle X\rangle$ vs. $\langle Z\rangle$ with variable P (P varies from 0 to 1 μM) for different total number of IP_3Rs channels: N=2 (dot), 20 (dash) and 200 (dash dot). The solid star is for the deterministic case (as same as the solid star in Fig. 2b). (b) The mean value of X as a function of the total channel number N at P=0.3 μM level (square), 0.5 μM (circle), 0.655 μM (star) and 0.8 μM (triangle), respectively.

phosphorylase, even if the mean level of Ca^{2+} (corresponding to the deterministic case) is below the threshold. Our results demonstrate that small number of IP_3R channel can potentiate the sensitivity of the activity of glycogen phosphorylase. An interesting extrapolation of our results is that the temporal evolution of cytosolic Ca^{2+} needs to be as deterministic as possible to avoid a 'preliminary' activation of the phosphorylase. In Fig. 6b, we have plotted the average fraction of active phosphorylase against the total IP_3R channel number increasing for different level of IP_3 stimuli. For the low concentration of IP_3 (e.g. P=0.3 μM), $\langle X\rangle$ is decreased as N increasing, however, for the high concentration level of IP_3 (e.g. P=0.8 μM), $\langle X\rangle$ is increased as N increasing. It should be pointed out that, when the total number of Ca^{2+} channel is very large (i.e. $N\rightarrow\infty$), the values of $\langle X\rangle$ for different P must tend to results for the deterministic case as shown in Fig. 2a.

The amplitude of X stochastic oscillations depends on the concentration of intracellular IP_3 and the total channel number. The various distribution for the amplitude of X in the P–N parameter plane is shown in Fig. 7a, which is a prediction by our computational simulations. There are five phase regions in this plane. When the IP_3 level is very low, the amplitude of X oscillations is smaller than 0.2, and concentrates on one value or several values, namely single-value region (indicated by I in Fig. 7a). Monotonically decreasing amplitude distributions are mainly found for low P level, namely monotonic-decrease region (indicated by II in Fig. 7a). When cluster has only a few IP_3Rs and P is approximately 0.4 μM, a dumbbell-like amplitude distribution (i.e. large probability occurs simultaneously in both the smallest X amplitude and the largest X amplitude) is observed (indicated by III in Fig. 7a). One-peak amplitude distributions are mainly found for medium P level (indicated by IV in Fig. 7a). For large P level, monotonically increasing amplitude distributions are observed in region V. In regions I, II, IV and V, the value of N does not influence the shape of X amplitude distributions. In Fig. 7b–e, we show four typical amplitude distribution forms corresponding to the points (b,c,d and e) as marked in Fig. 7a for different regions (except region I), respectively. The various distribution for the fraction of active glycogen phosphorylase presented here is similar to that for intracellular Ca^{2+} stochastic oscillations [22], and the puff amplitude distributions of cytosolic Ca^{2+} concentration have been observed

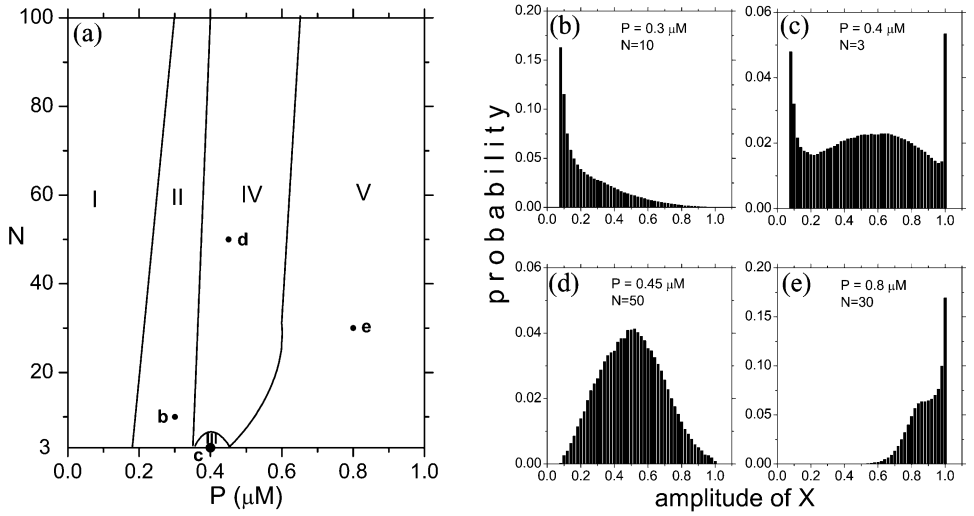

Fig. 7. (a) The Various distribution of the X amplitude in the $P-N$ parameter plane. Samples of the X amplitude distributions for points b, c, d, and e marked in various regimes are shown in (b)–(e), respectively.

in experiments from Xenopus oocytes and Hela cells [36–39].

4. Conclusions

In this article, by virtue of the Li–Rinzel model based on microscopic kinetics of IP_3 and Ca^{2+} gating of the IP_3R, we have studied theoretically the effects of both deterministic and stochastic intracellular Ca^{2+} oscillations on the regulation of a phosphorylation–dephosphorylation cycle process involved in glycogen degradation by glycogen phosphorylase *a*-form, respectively. In particular, we have explored theoretically the effects of different numbers of IP_3Rs and different levels of IP_3 stimuli on the activation of glycogen phosphorylase by stochastic cytosolic Ca^{2+} oscillations.

For the case of deterministic cytosolic Ca^{2+} oscillations, our results showed that the average fraction of active phosphorylase is increased with the concentration of intracellular IP_3 increasing, and that there exists an optimal frequency of cytosolic Ca^{2+} oscillations at which the average fraction of active glycogen phosphorylase reaches a maximum value. An interesting result is that the average fraction of active phosphorylase drops suddenly from high level to low value when the cytosolic Ca^{2+} oscillation is over. It implies that a mutation for the average fraction of active glycogen phosphorylase will occur at the higher bifurcation point of Ca^{2+} oscillations.

For the case of stochastic cytosolic Ca^{2+} oscillations, our results showed that the fraction of active phosphorylase is strongly affected by the number of IP_3R channel and the level of IP_3 concentration. The threshold of $\langle Z \rangle$ for activation of phosphorylase depends on the IP_3R channel number. The smaller the total number of Ca^{2+} channel is, the lower the threshold of $\langle Z \rangle$ for activation of phosphorylase is. Small number of IP_3R channel can potentiate the sensitivity of the activity of glycogen phosphorylase. Meanwhile, the average frequency and amplitude of stochastic oscillations in the fraction of active phosphorylase are increased with the level of IP_3 stimuli increasing. The various distribution for the amplitude of X stochastic oscillations in the $P-N$ parameter plane has been predicted, which shows that there are five possible shapes of amplitude distribution in the fraction of active glycogen phosphorylase.

Acknowledgements

The authors are very grateful to the two anonymous referees for the valuable comments and suggestions. This work was supported by the National

Natural Science Foundation of China under Grant No. 10275026.

References

[1] A.H. Cornell-Bell, S.M. Finkbeiner, M.S. Cooper, S.J. Smith, Glutamate induces calcium waves in cultured astrocytes: long-range glial signaling, Science 47 (1990) 470–473.

[2] V.A. Golovina, M.P. Blaustein, Spatially and functionally distinct Ca^{2+} stores in sarcoplasmic and endoplasmic reticulum, Science 275 (1997) 1643–1648.

[3] P.D. Koninck, H. Schulman, Sensitive of CaM kinase II to the frequency of Ca^{2+} oscillations, Science 279 (1998) 227–230.

[4] R.E. Dolmetsch, K. Xu, R.S. Lewis, Calcium oscillations increase the efficiency and specificity of gene expression, Nature 392 (1998) 933–936.

[5] G.J. Allen, S.P. Chu, K. Schumacher, C.T. Shimazaki, D. Vafeados, A. Kemper, et al, Alteration of stimulus-specific guard cell calcium oscillations and stomatal closing in Arabidopsis det3 mutant, Science 289 (2000) 2338–2342.

[6] D. Gall, E. Baus, G. Dupont, Activation of the liver glycogen phosphorylase by Ca^{2+} oscillations: a theoretical study, J. Theor. Biol. 207 (2000) 445–454.

[7] M.L. Cárdenas, A. Goldbeter, The glucose induced switch between glycogen phosphorylase and glycogen synthase in the liver: outlines of theoretical approach, J. Theor. Biol. 182 (1996) 421–426.

[8] A. Rozi, Y. Jia, A theoretical study of effects of cytosolic Ca^{2+} oscillations on activation of glycogen phosphorylase, Biophys. Chem. 106 (2003) 193–202.

[9] S.S. Stojilkovic, T. Iida, F. Merelli, A. Torsello, L.Z. Krsmanovic, K.J. Catt, Interactions between calcium and protein kinase C in the control of signaling and secretion in pituitary gonadotrophs, J. Biol. Chem. 266 (1991) 10377–10384.

[10] S.S. Stojilkovic, M. Kukulian, M. Tomic, E. Rojas, K.J. Catt, Mechanism of agonist-induced $[Ca^{2+}]_i$ oscillations in pituitary gonadotrophs, J. Biol. Chem. 268 (1993) 7713–7720.

[11] K. Kuba, S. Nishi, Rhythmic hyperpolarizations and depolarization of sympathetic ganglion cells induced by caffeine, J. Neurophysiol. 39 (1976) 547–563.

[12] D.Lipscombe,D.V.Madison,M.Poenie,H.Reuter,R.W.Tsien,Tsien, Tsien, R.Y. Tsien, Imaging of cytosolic Ca^{2+} transients arising from Ca^{2+} stores and Ca^{2+} channels in sympathetic neurons, Neuron 1 (1988) 355–365.

[13] D.D. Friel, R.W. Tsien, Phase-dependent contributions from Ca^{2+} entry and Ca^{2+} release to caffeine-induced $[Ca^{2+}]_i$ oscillations in bullfrog sympathetic neurons, Neuron 8 (1992) 1109–1125.

[14] H. Cheng, W.J. Lederer, M.B. Cannel, Calcium sparks: elementary events underlying excitation–contraction coupling in heart muscle, Science 262 (1993) 740–744.

[15] N. Callamaras, J.S. Marchant, X. Sun, I. Parker, Activation and co-ordination of $InsP_3$-mediated elementary Ca^{2+} events during global Ca^{2+} signals in Xenopus oocytes, J. Physiol. 509 (1998) 81–91.

[16] N. Melamed-Book, S.G. Kachalsky, I. Kaiserman, R. Rahamimoff, Neuronal calcium sparks and intracellular calcium 'noise', Proc. Natl. Acad. Sci. USA 26 (1999) C15217–C15221.

[17] A. Gonzalez, W.G. Kirsch, N. Shirokova, G. Pizarro, G. Brum, I.N. Pessah, et al, Involvement of multiple intracellular release channels in calcium sparks of skeletal muscle, Proc. Natl. Acad. Sci. USA 97 (2000) 4380–4385.

[18] D.D. Mak, S. Mcbride, J.K. Foskett, Regulation by Ca^{2+} and inositol 1,4,5-trisphosphate ($InsP_3$) of single recombinant type 3 $InsP_3$ receptor channels: Ca^{2+} activation uniquely distinguishes types 1 and 3 $InsP_3$ receptors, J. Gen. Physiol. 117 (2001) 435–446.

[19] G.W. De Young, J. Keizer, A single-pool inositol 1,4,5-triphosphate-receptor-based model for agonist-stimulated oscillations in Ca^{2+} concentration, Proc. Natl. Acad. Sci. USA 89 (1992) 9895–9899.

[20] Y. Li, J. Rinzel, Equations for $InsP_3$ receptor-mediated $[Ca^{2+}]_i$ oscillations derived from a detailed kinetic model: a Hodgkin–Huxley like formalism, J. Theor. Biol. 166 (1994) 461–473.

[21] A.L. Hodgkin, A.F. Huxley, A quantitative description of membrane current and its application to conduction excitation in nerve, J. Physiol. 117 (1952) 500–544.

[22] J.W. Shuai, P. Jung, Stochastic properties of Ca^{2+} release of inositol 1,4,5-trisphosphate receptor clusters, Biophys. J. 83 (2002) 87–97.

[23] M. Bollen, S. Keppens, W. Stalmans, Specific features of glycogen metabolism in the liver, Biochem J. 336 (1998) 19–31.

[24] P. Cohen, A. Burchell, J.G. Foulkes, P.T.W. Cohen, T.C. Vanaman, A.C. Nairn, Identification of the Ca^{2+}-dependent modulator protein as the fourth subunit of rabbit skeletal muscle phosphorylase kinase, FEBS Lett. 92 (1978) 287–293.

[25] J. Keizer, G.D. Smith, Spark-to-wave transition: saltatory transmission of calcium waves in cardiac myocytes, Biophys. Chem. 72 (1998) 87–100.

[26] S. Swillens, G. Dupont, L. Combettes, P. Champeil, From calcium blips to calcium puffs: theoretical analysis of the requirements for interchannel communication, Proc. Natl. Acad. Sci. USA 96 (1999) 13750–13755.

[27] S.P. Dawson, J. Keizer, A single-pool inositol 1,4,5-trisphosphate-receptor-based model for agonist-stimulated oscillations in Ca^{2+} concentration, Proc. Natl. Acad. Sci. USA 96 (1999) 6060–6063.

[28] I.I. Moraru, E.J. Kaftan, B.E. Ehrlich, J. Watras, Regulation of type 1 inositol 1,4,5-trisphosphate-gated calcium channels by $InsP_3$ and calcium: simulation of single channel kinetics based on ligand binding and electrophysiological analysis, J. Gen. Physiol. 113 (1999) 837–849.

[29] M. Falcke, L. Tsimring, H. Levine, Stochastic spreading of intracellular Ca^{2+} release, Phys. Rev. E 62 (2000) 2636–2643.

[30] M. Bar, M. Falcke, H. Levine, L.S. Tsimring, Discrete stochastic modeling of calcium channel dynamics, Phys. Rev. Lett. 84 (2000) 5664–5667.

[31] E. Skaugen, L. Walløe, Firing behavior in a stochastic nerve membrane model based upon the Hodgkin–Huxley equations, Acta. Physiol. Scand. 107 (1979) 343–363.

[32] B. Hille, Ionic Channels of Excitable Membrane, 2nd ed, Sinauer Associate, Sunderland, MA, 1992.
[33] A.F. Strassberg, L.J. Defelice, Limitations of the Hodgkin–Huxley formalism: effects of single channel kinetics on transmembrane voltage dynamics, Neural Comp. 5 (1993) 843–855.
[34] A. Goldbeter, D.E. Koshland, An amplified sensitivity arising from covalent modification in biological systems, Proc. Natl. Acad. Sci. USA 78 (1981) 6840–6844.
[35] G. Dupont, A. Goldbeter, Protein phosphorylation driven by intracellular calcium oscillations: a kinetic analysis, Biophys. Chem. 42 (1992) 257–270.
[36] X. Sun, N. Callamaras, J.S. Marchant, I. Parker, A continuum of $InsP_3$-mediated elementary Ca^{2+} signaling events in Xenopus oocytes, J. Physiol. 509 (1998) 67–80.
[37] D. Thomas, P. Lipp, M.J. Berridge, M.D. Bootman, Hormone-evoked elementary Ca^{2+} signals are not stereotypic, but reflect activation of different size channel clusters and variable recruitment of channels within a cluster, J. Biol. Chem. 273 (1998) 27130–27136.
[38] J.S. Marchant, I. Parker, Role of elementary Ca^{2+} puffs in generating repetitive Ca^{2+} oscillations, EMBO J. 20 (2001) 65–76.
[39] L. Haak, L. Song, T.F. Molinski, I.N. Pessah, H. Cheng, J.T. Russell, Sparks and puffs in oligodendrocyte progenitors: cross talk between ryanodine receptors and inositol triphosphate receptors, J. Neurosci. 21 (2001) 3860–3870.